

Supplementary Information

Force-Induced Retro-Click Reaction of Triazoles Competes with Adjacent Single-Bond Rupture

Tim Stauch and Andreas Dreuw

*Interdisciplinary Center for Scientific Computing, Im Neuenheimer Feld 205, 69120 Heidelberg,
Germany*

Contents

Influence of linker length on rupture force and energy	S3
Total strain in 1,5-substituted triazoles	S5
JEDI analyses of the BOMD simulations with a gradually applied force	S6
BOMD simulations with a suddenly applied force.....	S7
References	S9

Influence of linker length on rupture force and energy

The presence of a linker changes the rupture force (F_{\max}) and the rupture energy (E_{\max}) in a nontrivial manner. In Figure S1, the influence of the linker length on F_{\max} and E_{\max} is shown for the coordinates **c5-c7** and the 1,4- and 1,5-substitution patterns.

In the case of the symmetric stretching coordinate **c5**, 1,5-substitution of the triazole ring slightly increases F_{\max} . Initially, E_{\max} increases as well, but the effect becomes negligible and is eventually reversed as the linker gets longer. A pronounced opposite effect is found for the 1,4-substitution pattern: The presence of a linker decreases F_{\max} and E_{\max} , although the impact on E_{\max} is dampened by a long linker.

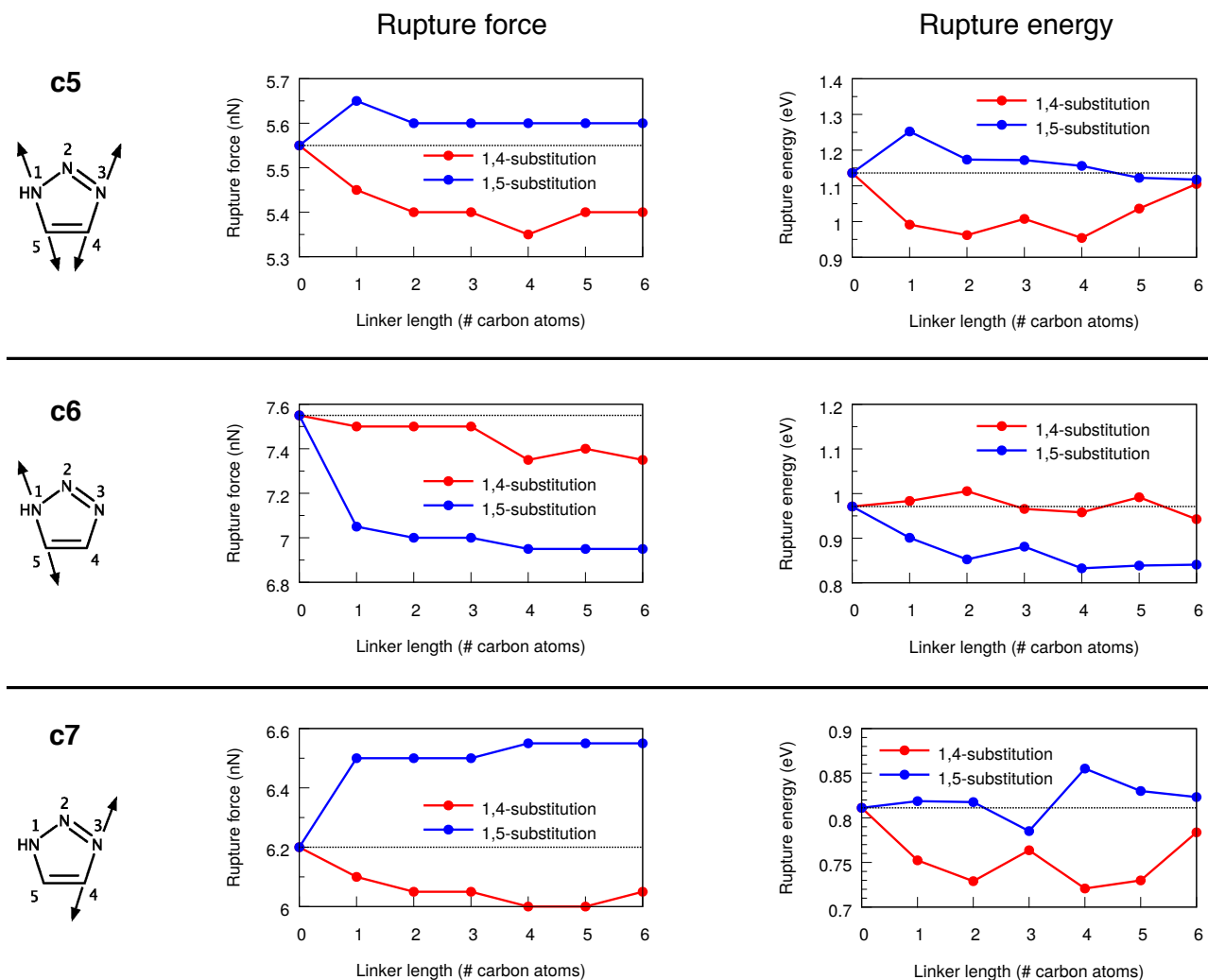


Figure S1: Rupture force F_{\max} (left column) and rupture energy E_{\max} (right column) of the stretching coordinates **c5-c7** as a function of linker length. Lines are included to guide the eye. The rupture forces and energies of the unsubstituted triazole rings are included as dashed lines. MarvinSketch was used for drawing the chemical structures.¹

A different behavior is found for the unzipping coordinate **c6**. Here, 1,5-substitution decreases F_{\max} and E_{\max} tremendously, but the length of the linker plays only a secondary role. 1,4-substitution leads to a slight decrease in F_{\max} , whereas E_{\max} hardly changes.

The influence of a linker on the second unzipping coordinate **c7** resembles the behavior observed for **c5**: 1,5-substitution increases F_{\max} and E_{\max} (except for the propyl linker), whereas 1,4-substitution decreases these quantities.

In summary, substitution of the triazole ring at an atom that is involved in the bond that is initially ruptured (the N3–C4 bond in **c5** and **c7** and the N1–C5 bond in **c6**) usually decreases F_{\max} and E_{\max} . This demonstrates that the linker has an electronic influence on the triazole ring and can potentially enhance cycloreversion not only by transmitting mechanical energy.

In many cases we observed that the potential energy surfaces of the triazole rings are shallow in the direction of the stretching of the two N–C bonds and exhibit at least two separate minima in each case. We observed that stretching the N–C bonds with the EFEI method starting from the relaxed geometry results in a local minimum with a significantly elongated N–C bond. This minimum was found to be higher in energy than another minimum with a shorter N–C bond and resulted in an unreasonably high strain energy, as calculated with the JEDI analysis. The lower minimum with a shorter N–C bond was jumped over. These situations were encountered in five cases and measures were taken to converge to the lower minimum. These lower minima are shown in Figure S1. In the case of the stretching coordinate **c5** and a 1,4-substitution with a propyl linker, the N3–C4 bond length was initially set to 1.63 Å and the N1–C5 bond length was set to 1.53 Å. In addition, the maximum allowed step size in the geometry optimization was adjusted to 0.01 a.u.. Subsequently, a conventional EFEI calculation was carried out. To converge to the lower minimum in the case of **c6** with 1,4- and 1,5-substitution with a propyl linker, the EFEI calculation started from a geometry in which the N1–C5 bond length was adjusted to 1.65 Å. In the **c7** coordinate with 1,5-substitution with a butyl linker, the N3–C4 bond length was adjusted to 1.65 Å initially, and in the case of a 1,4-substitution with a hexyl linker the same bond length was set to 1.64 Å initially and the displacement tolerance of the geometry optimization was set 0.003 a.u..

Total strain in 1,5-substituted triazoles

In Figure S2, the total amount of strain energy ΔE_{DFT} in 1,5-substituted triazoles immediately prior to rupture upon stretching end-to-end is shown. The strain energy increases linearly with the chain length, since adding an additional methylene group at each linker leads to the generation of a fixed amount of additional internal coordinates. Thus, adding a methylene group on each side of the molecule increases the amount of strain energy stored in the system by 0.945 eV (rss = 0.003 eV).

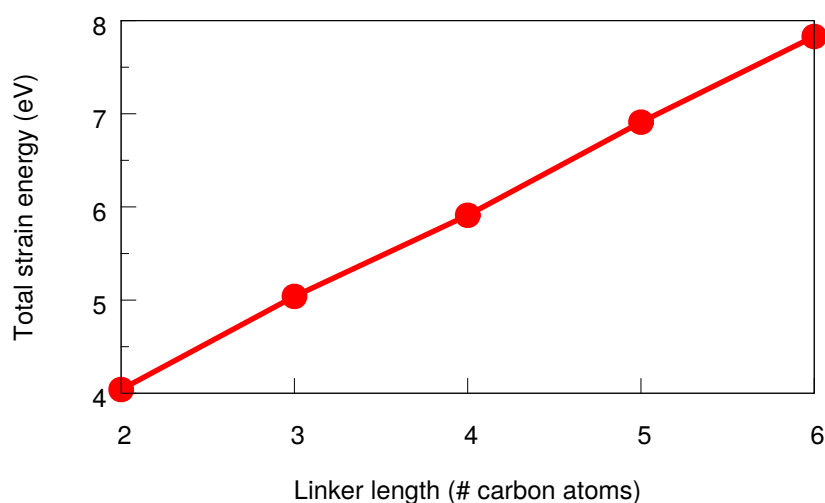


Figure S2: Total strain energy of 1,5-substituted triazoles with linkers of different sizes immediately prior to rupture upon stretching end-to-end. Lines are included to guide the eye.

JEDI analyses of the BOMD simulations with a gradually applied force

JEDI analyses were conducted for each of the ten BOMD simulations with a loading rate of 10^9 nN/s (Figure S3). To this end, the geometries of 500 consecutive simulation steps were averaged in order to minimize the influence of random thermal vibrations on the results of the JEDI analysis. These mean geometries were taken as the mechanically strained structures and the potential energies were calculated. The evolution of the energies during the BOMD simulations mirrors the temporal progression of the bond lengths. The energies in the bonds N1–C5, N1–C6 and C5–C7 generally increase during the trajectories. As soon as a bond is ruptured, anharmonic effects become dominant and the error of the harmonic approximation results in a sharp rise in potential energy. This effect can be observed eight times for the bond N1–C5 (resulting from eight cycloreversions) and two times for the bond N1–C6 (resulting from two rupture events of this interface bond). While the results of the JEDI analysis are no longer quantitative as soon as a bond is ruptured, the similarity of the energies in the bonds N1–C5 and N1–C6 up to this point explains quantitatively why both bonds have a significant rupture probability.

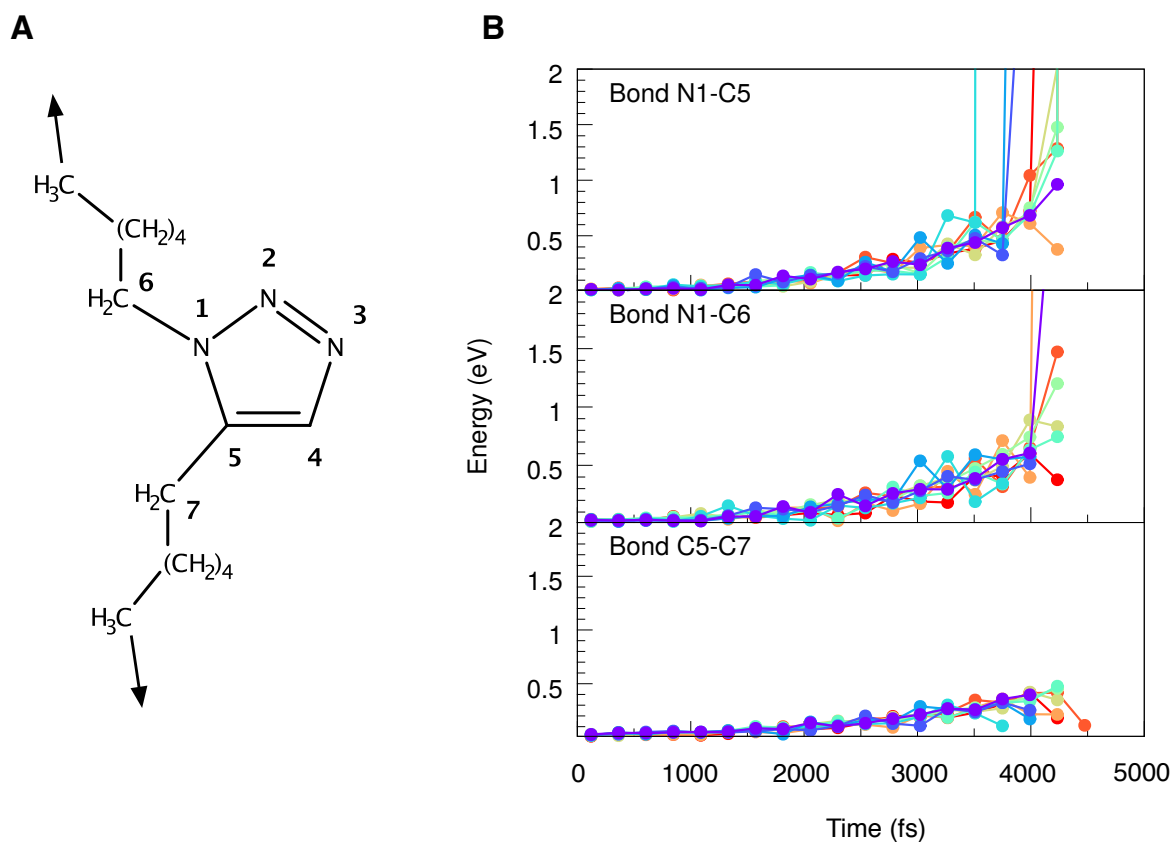


Figure S3: A: Numbering scheme and stretching coordinate used in the BOMD simulations with a loading rate of 10^9 nN/s. B: Potential energies stored in the bonds N1–C5, N1–C6 and C5–C7, calculated with the JEDI analysis for each of the ten BOMD trajectories. Each line represents one BOMD trajectory.

BOMD simulations with a suddenly applied force

In a separate set of BOMD simulations, the force was applied suddenly to 1,5-substituted triazole with hexyl linkers and the temperature was set to 0K, so that the JEDI analysis can be carried out at each time step.² Hence, the nuclear motion is only a result of the stretching and each time step yields a mechanically deformed geometry. A total of 5000 time steps (0.484 fs each) was calculated, so that the total simulation time amounted to 2.42 ns.

The end-to-end distance as well as the bond lengths N1–C5, N1–C6 and C5–C7 at different stretching forces as a function of simulation time are shown in Figure S4A. The end-to-end distances exhibit oscillatory behavior. At moderate forces (2.1 and 2.2 nN), these oscillations can be observed throughout the entire simulation time. At larger forces, cycloreversion occurs shortly after the third oscillation (2.3–2.5 nN) or almost instantaneously ($F \geq 2.6$ nN), resulting in a sharp increase in the end-to-end distance.

This behavior is reflected by the N1–C5 distances, but the time scale of the oscillations is much shorter. At moderate forces, the N1–C5 bond length oscillates during the entire simulation time, although the distance that is the rupture elongation in the static case is surpassed several times. This can be explained by the large-scale motion of the molecule as a whole, since the terminal carbon atoms are already “on their way back” when the N1–C5 bond length approaches its maximum. This leads to a momentary compression of the bond. Again, larger forces lead to dissociation.

The two interface bonds N1–C6 and C5–C7 oscillate during the entire simulation time, but never surpass their corresponding static bond rupture elongation. The N1–C6 bond, however, is generally closer to this value than the C5–C7 bond, which demonstrates once again that the carbon-nitrogen bonds in the molecule are the weak points. However, when a force is suddenly applied at 0K, we observed only cycloreversion and not rupture at the interface between the triazole ring and the linkers.

These findings can be rationalized by the dynamic JEDI analysis, in which the distribution of potential energy among the internal coordinates of the molecule is investigated in each time step. Since only the potential energy and not the kinetic energy is considered and the error of the harmonic approximation is not corrected, these results are qualitative. During the major part of the simulation with a stretching force of 2.3 nN, for example, most potential energy is stored in the N1–C5 bond (Figure S4C). Generally, the amount of energy in the N1–C6 bond is higher than in the C5–C7 bond. This observation agrees well with the temporal progression of the corresponding bond lengths. Shortly after 750 fs, the N1–C5 bond breaks, which is reflected in the sharply increasing energy resulting from strong anharmonic effects.

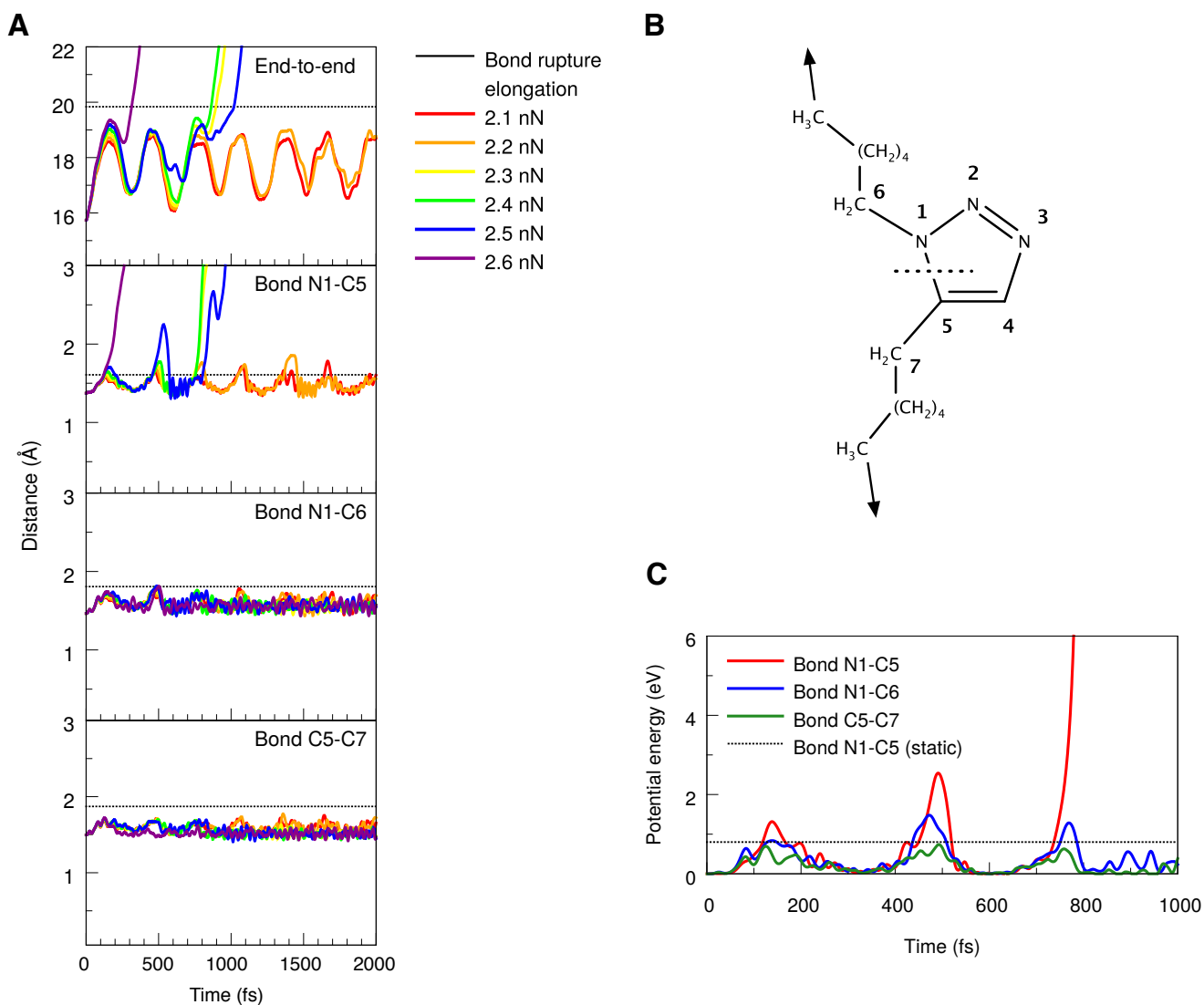


Figure S4: 1,5-substituted triazole with hexyl linkers was stretched end-to-end in a BOMD simulation at 0K. **A**: Various distances at forces between 2.1 and 2.6 nN are plotted against the simulation time. These include the end-to-end distance as well as the bond lengths N1–C5, N1–C6 and C5–C7. The distances at the point of bond rupture in static EFEI calculations are included as dotted lines. **B**: Numbering scheme and end-to-end-stretching coordinate of 1,5-substituted triazole. **C**: Potential energies stored in the bonds N1–C5, N1–C6 and C5–C7, calculated with the JEDI analysis for a force of 2.3 nN. The bond rupture energy of the N1–C5 bond, calculated with the static EFEI approach, is included as a dotted line.

Hence, these results are not quantitative, but support the qualitative interpretations that the N1–C5 bond is activated efficiently by a stretching force that is suddenly applied to the terminal carbon atoms and that the carbon-nitrogen bonds in the molecule are significantly weaker than the carbon-carbon bonds. Color-coded movies revealing the propagation of strain energy in the molecule and the activation of the N1–C5 bond are part of the Supporting Information.

The forces needed for cycloreversion in this setup are approximately half the forces required in the

BOMD simulations with a gradually applied force (see paper), since the molecule has only insufficient time to equilibrate and to redistribute the mechanical energy among its internal coordinates if the force is applied suddenly. This leads to rapid propagation of mechanical strain from the chain ends to the center, where constructive interference occurs. We hypothesize that it is possible to selectively trigger rupture at one of the bonds connecting the triazole ring to the linkers (preferably the N1–C6 bond) in BOMD simulations by shortening the linker on the opposite side of the molecule by one or two carbon atoms. In this case, the constructive interference would occur directly at the interface, thus leading to efficient rupture of the interface bond. Due to the size of the system and the high computational demands, however, such calculations were not carried out. Nevertheless, we conclude that a much higher loading rate would decrease the required rupture forces. At the same time, the selectivity observed here can hardly be expected in experiments, since the probability of rupture follows a Gaussian distribution and is highest in the central 15% of the chain.^{3,4}

References

- [1] ChemAxon (<http://www.chemaxon.com>), *Marvin*, 2017.
- [2] T. Stauch and A. Dreuw, *Acc. Chem. Res.*, 2017, DOI: 10.1021/acs.accounts.7b00038.
- [3] P. A. R. Glynn, B. M. E. van der Hoff and P. M. Reilly, *J. Macromol. Sci. Part A Pure Appl. Chem.*, 1972, **6**, 1653–1664.
- [4] P. A. R. Glynn and B. M. E. van der Hoff, *J. Macromol. Sci. Part A Pure Appl. Chem.*, 1973, **7**, 1695–1719.